Hindawi
Mathematical Problems in Engineering
Volume 2022, Article ID 4418706, 12 pages
https://doi.org/10.1155/2022/4418706

Research Article

E-dyNSGA-III: A Multi-Objective Algorithm for Handling Pareto Optimality over Time

Ima Okon Essiet,[1] **Yanxia Sun**,[1] **and Zenghui Wang**[2]

[1]*Department of Electrical and Electronic Engineering Science, University of Johannesburg, Johannesburg, South Africa*
[2]*Department of Electrical Engineering, University of South Africa, Pretoria, South Africa*

Correspondence should be addressed to Zenghui Wang; wangzengh@gmail.com

Received 14 March 2022; Revised 15 May 2022; Accepted 27 May 2022; Published 17 June 2022

Academic Editor: Hui Wang

Loss of selection pressure in the presence of many objectives is one of the pertinent problems in evolutionary optimization. Therefore, it is difficult for evolutionary algorithms to find the best-fitting candidate solutions for the final Pareto optimal front representing a multi-objective optimization problem, particularly when the solution space changes with time. In this study, we propose a multi-objective algorithm called enhanced dynamic non-dominated sorting genetic algorithm III (E-dyNSGA-III). This evolutionary algorithm is an improvement of the earlier proposed dyNSGA-III, which used principal component analysis and Euclidean distance to maintain selection pressure and integrity of the final Pareto optimal front. E-dyNSGA-III proposes a strategy to select a group of super-performing mutated candidates to improve the selection pressure at high dimensions and with changing time. This strategy is based on an earlier proposed approach on the use of mutated candidates, which are randomly chosen from the mutation and crossover stages of the original NSGA-II algorithm. In our proposed approach, these mutated candidates are used to improve the diversity of the solution space when the rate of change in the objective function space increases with respect to time. The improved algorithm is tested on RPOOT problems and a real-world hydrothermal model, and the results show that the approach is promising.

1. Introduction

Handling an increasing number of objectives over time is one of the challenges of evolutionary algorithms (EAs). In particular, handling problems with many objectives and complicated Pareto optimal front can impact the performance of EAs negatively. The idea of Pareto dominance with respect to any two solutions a and b of a many-objective optimization problem is guided by the following (where solution a dominates solution b): (i) solution a completely dominates solution b after the natural selection process; (ii) both solutions are infeasible, but solution a has a smaller constraint violation than solution b with respect to the objective function; and (iii) solution a is feasible, while solution b is infeasible [1]. Pareto dominance is straightforward to implement when the number of objectives is not greater than 3. However, with more than 3 objectives, it becomes difficult to select the final set of solutions that satisfy all objectives describing the problem.

When we consider Pareto optimality in the presence of changing time, there is an additional uncertainty that is introduced since a given solution selected at instant t_1 may not satisfy the problem at instant t_2. Also, there is a possibility that a given solution at t_1 will still be effective at t_2. However, the changing solution space over time might cause these fit solutions to be lost because of loss of selection pressure at high dimensions. Therefore, improving the performance of EAs to effectively handle Pareto optimality over time in the presence of many conflicting objectives is imperative. In this study, we present a multi-objective optimization algorithm called enhanced dynamic non-dominated sorting genetic algorithm III (E-dyNSGA-III). It is originally based on the NSGA-III algorithm [2] and is an improvement on an earlier proposed dynamic multi-

objective evolutionary algorithm (DMOEA) called dyNSGA-III [3]. The aim of the proposed improvement is to enhance the performance of dyNSGA-III on the optimization of robust Pareto optimality over time (RPOOT) problems and a multi-objective real-world power scheduling problem. RPOOT problems consist of dynamic Pareto set (PS) and Pareto front (PF) with respect to time [4]. The proposed E-dyNSGA-III algorithm uses a strategy to select and maintain a group of top-performing, mutated, and randomly chosen candidate solutions in the population in the presence of multiple objectives. In particular, these mutated solutions help to maintain the diversity of the Pareto front when there is a frequent change in objective function(s), constraint functions, and/or variable boundaries representing a given dynamic many-objective optimization problem (DMOP). These candidate solutions help to maintain the selection pressure of the EA as much as possible even in high dimensionality.

The main contribution of this study is to use randomly generated mutated solutions from a reference point-based search strategy to improve the selection pressure of dyNSGA-III when the number of objectives is 3 or greater and/or when the DMOP has several dynamic parameters and constraints.

The rest of the study is organized as follows: Section 2 describes the use of evolutionary algorithms in multi-objective optimization. Section 3 outlines the proposed methodology for implementing E-dyNSGA-III for dynamic multi-objective optimization and discusses the test results obtained from using E-dyNSGA-III to optimize 4 selected instances of 3-objective, dynamic many-objective optimization problems (DMOPs). Obtained results are compared with an earlier proposed dyNSGA-III algorithm. We then compare the performance of E-dyNSGA-III with 2 other well-performing DMOEAs for dimensionality reduction in the presence of many objectives. We also present a multi-objective model of a power generation scheduling problem and optimize it using both E-dyNSGA-III and dyNSGA-III. The results are also discussed. Section 4 concludes the study.

2. Many-Objective Optimization Using Evolutionary Algorithms

Several real-world problems are best modelled as many-objective optimization problems such as power system stability [5], induction motor design [6], radar-absorbing material design [7], and job-shop scheduling [8]. Therefore, several researchers have proposed various methods of improving the performance of EAs to effectively balance convergence and diversity in the presence of many conflicting objectives with rapidly changing Pareto fronts. In [9], the robust ranking and selection approach for handling intractable complex optimization considering randomness was reformulated as a multi-objective ranking and selection problem. In this case, a single ranking and selection problem is decomposed into several objectives. In [10], a cache approach was proposed to improve the balance between convergence and diversity in the presence of high dimensionality, thus improving selection pressure, while [11] proposed a two-stage strategy and parallel cell coordinate system (PCCS) to remedy the same problem.

In [12], the test case generation problem was modelled as a dynamic many-objective optimization problem instead of the popular single-objective problem. A dynamic many-objective sorting algorithm (DynaMOSA) was proposed to solve the proposed optimization problem, and it was observed that this approach outperformed single-objective optimizers by 28%. Further research has focused on improving evolutionary and nature-inspired algorithms to tackle challenges of many objectives characterizing real-world problems [13], minimizing impact of expensive feature evaluations [14], and improving selection pressure [15]. A hybridized minimal cost evolutionary deterministic algorithm (HMCEDA) was one of the first evolutionary algorithms used to solve DMOPs [16]. The algorithm was used to optimize 5 DMOPs with slowly changing environments. Dynamic particle swarm optimization (DPSO) algorithm has also been proposed in [17] to solve DMOPs using Pareto dominance with hyperplane distribution. DPSO handles changes in the search environment by adjusting the velocity parameter of PSO for previous non-dominated candidates.

The immune optimization approach has been used in recent years as a solution to DMOPs. In particular, the interaction between B and T cells was used to create an artificial immune system (AIS) approach for tracking DMOPs [18]. Also, an immune surveillance approach was proposed for solving such problems in [19]. A recent approach combined AIS-based clonal selection with generalized differential evolution 3 (GDE3) algorithm to solve DMOPs. In [20], a distributed population evolution strategy based on the message passing interface (MPI) approach was used to optimize several DMOPs of the generalized dynamic benchmark generator (GDBG). The proposed algorithm was based on a multi-population, cloud-based variant of the differential evolution algorithm called Cloudde. It is clear to see that more real-world problems are modelled as many-objective optimization problems. Therefore, it is important to improve the capability of EAs to effectively solve this problem. The next section details the proposed approach to preserve the quality of selected solutions and pull selected solutions as close as possible to the Pareto front.

3. Proposed Methodology

In this section, we will discuss the elite archive approach that we apply to improve the capability of dyNSGA-III to handle dynamic search spaces involving 3 or more objectives. In dyNSGA-III, we used adaptive principal component analysis (PCA) mutation with n-point crossover to improve the ability of NSGA-III to track the PF in dynamic environments [3]. Adaptive PCA selects features with the highest covariance in high-dimensional environments, while n-point crossover increases the degree of randomness of selection of offspring of successive generations. Therefore, this results in a sustained balance of convergence and diversity in a search space involving up to 3 objectives. For up to 2 objectives with few parameter and constraint variations, the selection strategy by dyNSGA-III is maintained. However, for 3 or

more objectives, a selection strategy similar to the elite NSGA-III approach is used. However, in our proposed algorithm (Algorithm 1), we increase the number of reference points and elite solutions to compensate for the effects of both changing space and time as the number of objectives increases. In particular, we consider two situations: when there is a small change in the problem with respect to time and when there is a large change. In both situations, we would examine the effect of introducing varying proportions of mutated solutions into the OF space on the ability of the DMOEA to arrive at the best possible solution to the DMOP. It is important to consider these two scenarios with respect to time because while frequent changes in small magnitude can result in not enough time to find a suitable solution or set of solutions to the problem, less frequent changes in comparatively larger magnitude can result in the best solutions being traded for less fit candidates. Therefore, it is important to ensure the best possible trade-off between both cases.

For Algorithm 1, we use the maximum Euclidean distance with respect to initial population and the final covariance matrix to evaluate the fitness of the elite population representing the non-dominated PF. The covariance matrix Γ_{cov} is obtained according to

$$\Gamma_{cov} = \alpha\left((\boldsymbol{\sigma} - \alpha(\boldsymbol{\sigma}))\left(\boldsymbol{\sigma} - \alpha(\boldsymbol{\sigma})^{\mathbf{T}}\right)\right), \tag{1}$$

where σ is matrix of points within n-dimensional Euclidean space and $\alpha(\sigma)$ is mean value.

The solution space from which the set of elites is selected is centered with respect to selected reference points using PCA according to

$$\mathbf{R} = (\boldsymbol{\sigma} - \alpha(\boldsymbol{\sigma}))\Delta\vartheta, \tag{2}$$

where ϑ is the matrix of eigenvectors.

This approach maintains the elite population effectively for problems that have 2 objectives. However, for more than 3 objectives, we modify the number of reference points by $2^M - 1$, where M is the number of objectives. To determine the rate of change in the given problem solution space, we consider the Minkowski distance $D_M(x, y)$ of solution a from its associated reference point at time t_n and t_{n+1}, respectively. If the change in $D_M(x, y)$ is large, then rate of change is large for solution a. Otherwise, the rate of change is considered to be small. For a small rate of change in the presence of 3 or more objectives, we infer that more competition is required to obtain the fittest candidates. Therefore, we introduce a larger proportion of mutated solutions according to the number of reference points. For instance, if a small change is detected, we introduce 2^M mutated solutions for every reference point. Otherwise, if the change is large, we increase the number of reference points by $2^M - 1$ to guide the population to Pareto optimality. The assumption here is that for large changes in the solution space, premature convergence is unlikely.

When the objectives are more than 2, the number of reference points and elite solutions is increased by a factor of $2^M - 1$, where M is the number of objectives. We recognize that parent selection can result in loss of selection pressure and diversity among the solutions. However, the archived approach has demonstrated improved performance [21, 22].

From steps 5 and 6 of Algorithm 1, we attempt to cater for changes in both space and time as the number of objectives and dimensions increases. This is because NSGA-III typically loses selection pressure as the number of objectives increases. Steps 5 and 6 of the algorithm are the main contribution of this research to improve the performance of earlier proposed dyNSGA-III algorithm. We believe that this modified selection and orientation of reference points in the objective function space would push fit and relevant solutions towards the Pareto optimal front. The Minkowski distance is used as the metric to ensure the proper spread of candidate solutions. The Minkowski distance between two points x and y is obtained as follows:

$$D_M(x, y) = \left(\sum_{i=1}^{n} |x_i - y_i|^m\right)^{1/m}, \tag{3}$$

where m is the order of the norm.

The Minkowski distance metric ensures that the elite population P_e contains not only the candidates closest to the ideal point but also those close to these ideal candidates. It is a generalized form of the Euclidean distance and Manhattan distance metrics. This would ensure that the archive not only contains the best candidates, but also a number of "second" best candidates. Thus, the fitness of the archive is maintained. The purpose of such a strategy is to ensure that solutions that may have been discarded are preserved until later generations till the stopping criterion (max_gen) is reached. The suitability and durability period of candidate solutions are described according to the following equations.

$$f_a(\mathbf{x}, t) = \frac{1}{T}\sum_{j=0}^{T-1} f_{a,b+j}(\mathbf{x}), \tag{4}$$

$$t_s(\mathbf{x}, t) = \begin{cases} \Delta 0 \; if \; f\_(a, t)(x) < F, \\ \Delta 1 + \max\{p, \quad \forall j \in t, t+1, \ldots, (t+p)\}, \\ \Delta \; if \; f_{a,t}(\mathbf{x}) \geq F. \end{cases} \tag{5}$$

Equations (4) and (5) are additional indices, which ensure that the elite solution archive remains fit with the increasing number of objectives under conditions of changing space and time.

Table 1 details the simulation parameters and settings for the dynamic environment. Table 2 gives details of the test cases used for determining the capability of E-dyNSGA-III to obtain robust solutions over time.

From Table 1, parameter settings are selected to be the same as those used for the original dyNSGA-III. We want to ensure that the simulation environment is maintained to get the best performance from the EA.

3.1. E-dyNSGA-III Optimization of RPOOT Problems. In this section, we discuss the performance of our proposed algorithm on selected RPOOT problems. The selected problems are multi-objective with complicated PF.

Input: reference points on normalized hyperplane P_r with specific location 1. . .. . $|P_r|$, parent population $n_{\text{pop},t}$, offspring population $n_{\text{pop},o,t}$, elite population P_e, distance of elite population to the ideal point P_i, max_gen = 500
Output: elite population $P_{e,t}$, updated reference point location with respect to ideal point $l_{\text{up ref},t}$
2009 while $M \leq 2$:
(1) Apply adaptive mutation strategy specified in (1) and (2)
(2) Obtain the set of elites P_e and current location of updated reference points
else if $M \geq 3$:
(3) Increase the number of reference points P_r by $2^M - 1$ and arrange in the normalized hyperplane by associating each member of $P_{e,t}$ with a reference point
(4) Execute step 1
(5) Obtain set of elites P_e and current location of updated reference points according to: $[P_{e,t+1}, l_{\text{up ref},\, t+1}]$ = Update Elite($l_{\text{up ref},\, t}$, $P_{e,t}$,$n_{\text{pop},t}$,$n_{\text{pop},o,t}$)
(6) Compare current location of solutions with ideal Pareto front using Minkowski distance $D_M(x, y)$
End
End

Algorithm 1:

Table 1: Parameter settings.

Parameter	Setting
Problem dynamicity (s_t)	5 (initial)
Frequency of change (f_t)	10 (initial)
Dimension size	50
Number of population guiding points (p_t)	21
Number of search candidates (N_s)	300 (for F_7 and F_8) 500 (for F_{10} and F_{11})
Mutation probability (p_m)	0.1
Crossover rate (c_r)	0.5 (adaptive)
Crossover distribution index (ρ_d)	28
Mutation distribution index (ρ_m)	15

From Table 2, test instances F_7, F_8, F_{10}, and F_{11} are robust Pareto optimality over time (RPOOT) test problems from [4]. They all consist of 3 time-dependent objective functions with dynamic Pareto set and Pareto front, respectively. Complexities of selected test problems are meant to test the ability of DMOEA to handle changing characteristics of the problems in the presence of changing time.

According to [16], F_7 is a type I DMOP with non-convex Pareto optimal front (POF), and F_8 is a type II DMOP with non-convex POF. Both DMOPs represent a continuous search space for the DMOEA with the rate of change in these problems being either gradual or sudden with time. From [23], F_{10} and F_{11} are described as unconstrained dynamic functions (UDFs). F_{10} has a simple trigonometric Pareto set, which is horizontal shifting with time. Its Pareto front is continuous with curvature change from convex to concave with angular shift with time. The search space has a dimension of $[0, 1] \times [-1, 1]^{n-1}$, where n is the number of dimensions of the search space. F_{11} is characterized by a trigonometric Pareto set with no associated dynamicity. The Pareto front is 3-dimensional and concave with time-shifting center and radius of the concave front. The search space has dimension of $[\theta]^2 \times [-2, 2]^{n-2}$. The Pareto front is discontinuous over the entire search space.

Indices for measuring the performance of E-dyNSGA-III include the duration of candidate survival (t_r), IGD (d_r), and spacing between non-dominated solutions (s_r). t_r is used to estimate how long fit solutions can remain relevant after successive generations. Therefore, the greater the survival time, the more likely ideal solutions are to be part of the final Pareto front. d_r indicates the spread of potential solutions of the given dynamic multi-objective optimization problem (DMOP). The smaller the magnitude of d_r, the better the spread of solutions in the objective function space. s_r measures the spacing between the final non-dominated set of solutions of the DMOP. This will ensure that the Pareto front is covered as much as possible by the final solution set. Mathematically, the indices are expressed as follows:

$$t_r = \frac{1}{T} \sum_{i=1}^{T} t_i, \tag{6}$$

where T is the period for which selected candidates remain suitable solutions for the DMOP and t_i is the period for which the ith Pareto solution is feasible.

$$d_r = \frac{1}{N} \sum_{i=1}^{N} \max_{k=k_{i_1},\ldots\ldots,k_{i_1+N_{k_i}}} \text{IGD}(k), \tag{7}$$

where N is the number of Pareto solutions and $\max_{k=k_{i_1},\ldots\ldots,k_{i_1+N_{k_i}}} \text{IGD}(k)$ is the inverted generational distance of the kth Pareto solution.

$$s_r = \frac{1}{N} \sum_{i=1}^{N} \left(\frac{1}{|\Psi(i)| - 1} \sum_{j=1}^{\Delta(i)} \left(\rho - \rho_k\right)^2 \right)^{1/2}, \tag{8}$$

where ρ_k is the least Euclidean distance between survival indices of the kth mutated solution in non-dominated front ($\Psi(i)$) and the Pareto front $\rho = \sum_{k=1}^{\Psi(i)} \rho_k$.

3.2. Results on E-dyNSGA-III Optimization of RPOOT Problems. From research done in [3], the original dyNSGA-III performed well on RPOOT problems. However, it struggled to find suitable solutions when the Pareto front was complicated, and the number of objectives was 3 or more. Therefore, in this study, we compare the performance of E-dyNSGA-III with dyNSGA-III for dynamic multi-

Table 2: RPOOT problem characteristics.

RPOOT problem	Characteristics
F_7: Farina-deb-amato 4 (FDA4) in [16]	3 time-dependent objective functions. Has dynamic non-dominated set and fixed Pareto front
F_8: FDA5 in [16]	3 time-dependent objective functions. Has dynamic non-dominated set and Pareto front
F_{10}: Unconstrained dynamic function 4 (UDF4) in [23]	3 time-dependent objective functions. Has dynamic non-dominated set and Pareto front
F_{11}: UDF7 in [23]	Has complicated Pareto optimal solutions with dynamic non-dominated set and Pareto front

Table 3: Performance comparison of dyNSGA-III and E-dyNSGA-II for selected DMOPs.

Test problem	Performance index	dyNSGA-III	E-dyNSGA-III
F_7	t_r	3.128 ± 0.046	3.773 ± 0.125
	d_r	1.275E-02(1.044E-01)	2.941E-03(1.742E-02)
	s_r	2.475E-03(2.631E-02)	2.803E-02(1.038E-01)
F_8	t_r	2.486 ± 0.312	2.941 ± 0.185
	d_r	2.165E-02(2.593E-02)	1.963E-03(2.106E-03)
	s_r	3.958E-02(1.128E-02)	2.851E-03(1.04E-03)
F_{10}	t_r	2.951 ± 0.093	3.307 ± 0.311
	d_r	3.753E-01(2.175E-01)	3.055E-03(2.951E-03)
	s_r	3.104E-02(1.198E-01)	2.619E-03(1.117E-02)
F_{11}	t_r	3.285 ± 0.175	4.042 ± 0.532
	d_r	2.952E-01(2.031E-02)	1.195E-03(2.584E-03)

objective optimization problems with 3 objectives and changing Pareto set and Pareto front.

From Table 3, it can be seen that the improved E-dyNSGA-III outperformed dyNSGA-III for the selected DMOPs with complicated and discontinuous Pareto front and Pareto set. The selected DMOPs also take into consideration the effect of changing time. However, we observe from t_r and d_r that E-dyNSGA-III is able to maintain fit solutions with the archive approach throughout successive generations of the search. For each algorithm, simulations were run 20 times to ensure proper convergence. s_r also indicates that candidate solutions are well spread across the Pareto front in the case of E-dyNSGA-III compared with dyNSGA-III.

To further compare the performance of dyNSGA-III and E-dyNSGA-III, we compare the percentage of runs in which each algorithm was able to associate specified reference points with at least one population member before the *max_gen* stopping criterion is attained. The idea behind this is to determine how effectively both algorithms use reference points to guide the population towards Pareto optimality. For $M = 3$, we set $max\_gen = 500$. From the results obtained in Table 4, it can be seen that E-dyNSGA-III is capable of associating a higher percentage of reference points with population candidates when the stopping criterion is satisfied. Figure 1 shows the ideal concave Pareto front for the F_7 3-objective type I DMOP.

From Figure 1, it can be seen that E-dyNSGA-III has a better approximation of the PF for F_7 as seen in Figure 1(b). The candidate solutions provide better coverage of the PF compared with dyNSGA-III (Figure 1(c)). The computational complexity of E-dyNSGA-III is $O(2N^2 \log^{M-2} N)$, which is approximately the same as that of dyNSGA-III. M is the dimensionality of the objective function, and N is the population size.

Table 4: Percentage of runs for which DMOEA is able to associate 90% of reference points with at least one population member for selected DMOP.

Test problem	dyNSGA-III (%)	E-dyNSGA-III (%)
F_7	76	79
F_8	88	90
F_{10}	83	89
F_{11}	80	85

From the results obtained, we observe that the proposed archive approach for handling DMOPs with more than 2 objectives is effective in handling up to three objectives for problems involving time-changing Pareto set and Pareto front. These attributes characterize many real-life problems, which are generally dynamic in nature.

3.3. Comparative Performance of E-dyNSGA-III on Selected Many-Objective DTLZ5 (x, y) Problems. In this section, we will compare the performance of E-dyNSGA-III with two other DMOEAs on their ability to eliminate redundant objectives in a case where the number of objectives is large. We will consider the DTLZ5 (x, y) problem set [24], where x represents the number of non-dominated objectives and y is the total number of objectives representing the DMOP. This DMOP tests the ability of E-dyNSGA-III to adapt to complex search environments, which characterize problems with many objectives. In particular, we test the ability of the algorithm to select non-dominated objectives out of the total number of objectives, thereby eliminating redundant objectives. This results in a simplification of the search space while simultaneously preserving the solutions required to solve the DMOP.

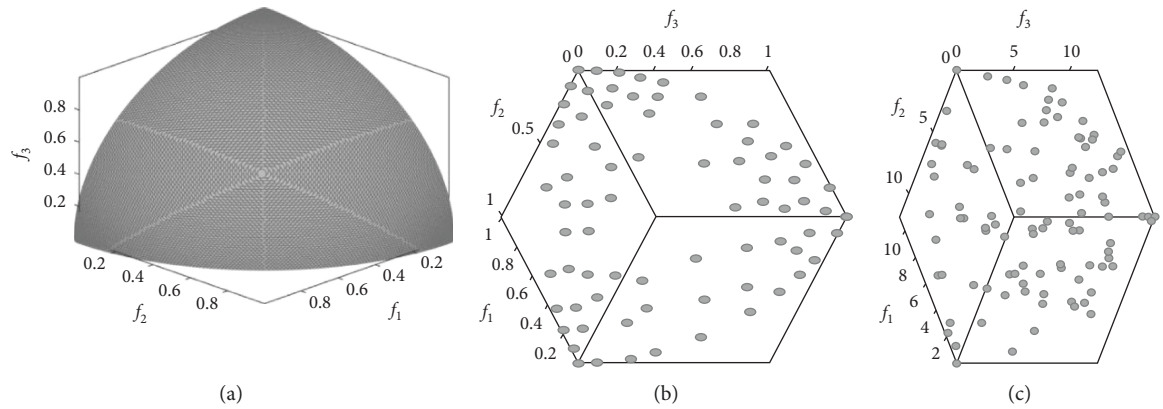

Figure 1: (a) Pareto front (PF) of F_7 DMOP. (b) E-dyNSGA-III PF approximation of F_7. (c) dyNSGA-III PF approximation of F_7.

The DTLZ5 (x, y) DMOP being considered include DTLZ5 (3,10) and DTLZ5 (5,10). We compare the performance of E-dyNSGA-III with two other DMOEAs: Pareto-PCA-NSGA-II [24] and Cloudde [20]. These DMOEAs were selected based on their promising performance with dimensionality reduction. In particular, E-dyNSGA-III and Pareto-PCA-NSGA-II use PCA for dimensionality reduction.

From the results obtained in Table 5, Pareto-PCA-NSGA-II and E-dyNSGA-III are the best performers for the lowest normalized Minkowski distance of selected solutions from the ideal PF (as indicated by the metrics highlighted in dark gray).

Pareto-PCA-NSGA-II has the lowest normalized Minkowski distance for DTLZ5 (3,10) after 100 iterations (0.3187) for objective F8, while E-dyNSGA-III has the lowest overall Minkowski distance for objective F3 after 100 iterations. This is important because it is a test of the algorithm's ability to push solutions as close as possible to the ideal PF despite the challenge of losing selection pressure in the presence of many objectives. Overall, E-dyNSGA-III achieved the lowest overall Minkowski distance for 5 objectives, while Pareto-PCA-NSGA-II achieved the lowest Minkowski distance for 4 objectives across all instances of DTLZ5 (x, y), for all iterations. It is important to note the role of PCA in dimensionality reduction for E-dyNSGA-III and Pareto-PCA-NSGA-II, which is likely the reason for their superior performance.

We also examine the ability of the algorithms to find non-dominated objectives as an indication of their capability to perform effective dimensionality reduction. Here, we consider specific instances of the DTLZ5 (x, y) test suite, across all iterations. From the results in Tables 5 and 6, we observe that E-dyNSGA-III achieves dimensionality reduction for 7 of 14 of the iterations for DTLZ5 (3, 10) and (5, 10) DMOPs (indicated by results highlighted in lighter shade of gray). The other 7 are distributed between Cloudde and Pareto-PCA-NSGA-II. This makes E-dyNSGA-III the best performer in terms of dimensionality reduction, which indicates that it is a promising candidate for tackling the problem of the curse of dimensionality associated with many DMOEAs as they try to optimize problems with many objectives. We observe that for all 3 DMOEAs, their search capability generally improves as the number of iterations increases. This is demonstrated by the decreasing value of the normalized Minkowski distance as the number of iterations increases between 100 and 1000 for both instances of DTLZ5 (3, 10) and (5, 10) considered.

3.4. Performance of E-dyNSGA-III on Multi-Objective Hybrid Power Generation Scheduling Model. In Section 3.1, we examined the performance of E-dyNSGA-III on the mathematical model of several time-varying multi-objective problems. Preliminary results show that E-dyNSGA-III performed better than an earlier proposed dyNSGA-III algorithm. We will now test the capability of our proposed algorithm to handle a multi-objective, real-world power generation scheduling model consisting of multiple energy sources.

The original problem was formulated as a hydrothermal power generation scheduling problem in [25]. The objective was to generate enough electricity to satisfy demand while minimizing generation cost and environmental emissions. This would also involve an optimal balance between the number of hydroelectric and thermal generating units required to satisfy these objectives and related constraints. The problem formulation is dynamic in nature due to the fact that the demand for power changes with time. Therefore, the DMOEA is expected to track new optimal solutions whenever problem parameters change. The dynamic problem formulation is detailed in (2) of [25] with a transmission loss term specified in (9). Parameters for the hydrothermal system are included in the appendix section of [25].

The dynamic nature of the problem formulation is simulated by considering an overall time window of 96 hours (4 days). We assume here that the DMOP and its associated parameters and constraints continually vary over time windows of varying durations as follows: 5 minutes, 10 minutes, 15 minutes, and 30 minutes. Therefore, we consider

Table 5: Minkowski distance values for DTLZ5(x,y) DMOPs.

Algorithm	Iterations	Objectives									
		F1	F2	F3	F4	F5	F6	F7	F8	F9	F10
Pareto-PCA-NSGA-II	100 (DTLZ5(3,10))	0.9547	0.7652	0.6383	0.7295	0.4873	0.5084	0.6215	**0.3187**	0.8540	0.3694
	DTLZ5(5,10)	0.8032	0.9173	0.7492	0.7916	0.5826	0.5919	0.4395	0.6184	0.6831	0.5948
	200 (DTLZ5(3,10))	0.8126	0.8957	0.7316	0.6386	0.5194	0.5397	0.5817	0.6217	0.6683	0.5726
	DTLZ5(5,10)	0.8316	0.9107	0.7528	0.6637	0.5859	0.6183	0.7046	0.6173	0.6974	0.6163
	400 (DTLZ5(3,10))	0.8051	0.8584	0.7437	0.5846	0.4983	0.5273	0.5428	0.6104	0.5936	0.5284
	DTLZ5(5,10)	0.8104	0.8861	0.6901	0.5917	0.5620	0.6054	0.6939	0.5818	0.6411	0.5749
	600 (DTLZ5(3,10))	0.8152	0.7763	0.7195	0.5405	0.4592	0.5196	0.5097	0.5828	0.5754	0.5127
	DTLZ5(5,10)	0.7973	0.8150	0.6635	**0.5235**	0.5229	0.5936	0.6306	0.5572	0.6049	0.5207
	800 (DTLZ5(3,10))	0.7773	0.7102	0.6936	0.5603	0.4726	0.5903	0.5761	0.5614	0.5419	0.4816
	DTLZ5(5,10)	0.7618	0.7954	0.6395	0.5404	0.5190	0.6105	0.6054	0.5072	0.5810	0.5503
	900 (DTLZ5(3,10))	0.7183	0.6937	0.6294	0.6919	0.4330	0.5729	0.4609	0.5337	0.5172	0.4405
	DTLZ5(5,10)	0.6641	0.7294	0.5803	0.5906	0.5021	0.6308	0.5992	0.4826	0.5319	0.4904
	1000 (DTLZ5(3,10))	0.6992	0.6407	0.6390	0.5607	**0.4118**	0.6517	**0.4349**	0.5185	0.4728	0.4239
	DTLZ5(5,10)	0.6390	0.6973	0.7294	0.5621	0.5137	0.6116	0.5621	0.4319	0.5185	0.4705
Cloudde	100 (DTLZ5(3,10))	0.8954	0.7385	0.7106	0.7216	0.7036	0.7130	0.6942	0.6284	0.7705	0.6106
	DTLZ5(5,10)	0.7720	0.7251	0.7518	0.7735	0.6219	0.6142	0.5184	0.6285	0.6617	0.6169
	200 (DTLZ5(3,10))	0.8626	0.7152	0.6930	0.8215	0.6961	0.7218	0.7105	0.6170	0.7384	0.6048
	DTLZ5(5,10)	0.7385	0.6943	0.7305	0.7280	0.6105	0.5992	0.6998	0.5883	0.6595	0.5972
	400 (DTLZ5(3,10))	0.8428	0.7164	0.6647	0.8006	0.6764	0.7162	0.6996	0.5964	0.7159	0.5885
	DTLZ5(5,10)	0.7168	0.6979	0.7206	0.7303	0.6007	0.5730	0.6994	0.5693	0.6501	0.5726
	600 (DTLZ5(3,10))	0.8247	0.7071	0.6482	0.7836	0.6831	0.6947	0.6996	0.5817	0.6992	0.5742
	DTLZ5(5,10)	0.6915	0.6385	0.7115	0.6931	0.5980	0.5594	0.6999	0.5884	0.6372	0.5638
	800 (DTLZ5(3,10))	0.7193	0.7002	0.6298	0.7528	0.6406	0.7274	0.6986	0.5717	0.6850	0.5318
	DTLZ5(5,10)	0.7753	0.6273	0.7096	0.6429	0.6005	0.5496	0.6958	0.5796	0.6674	0.5490
	900 (DTLZ5(3,10))	0.6974	0.6996	0.6499	0.7327	0.6217	0.7106	0.6983	0.5596	0.6969	0.5642
	DTLZ5(5,10)	0.7514	0.6151	0.6941	0.6140	0.5555	0.5165	0.6989	0.6063	0.6486	0.5276
	1000 (DTLZ5(3,10))	0.6736	0.6721	0.6295	0.7164	0.6003	0.6637	0.6973	0.5496	0.6741	0.5412
	DTLZ5(5,10)	0.6990	**0.5973**	0.6686	0.5976	0.5374	0.5326	0.6984	0.5995	0.6271	0.5184
E-dyNSGA-III	100 (DTLZ5(3,10))	0.8991	0.6383	**0.6283**	0.7548	0.4552	**0.4996**	0.6385	0.5135	0.7954	**0.3419**
	DTLZ5(5,10)	0.9063	0.7396	**0.7126**	0.6076	0.6021	**0.5591**	0.4417	**0.4157**	**0.6519**	**0.4886**
	200 (DTLZ5(3,10))	0.6503	0.7292	0.7614	0.6166	0.4962	**0.5288**	**0.6995**	**0.4007**	**0.6524**	**0.4527**
	DTLZ5(5,10)	0.7294	0.6149	**0.6337**	**0.6004**	**0.5916**	0.5184	**0.4406**	**0.5535**	0.7642	0.5001
	400 (DTLZ5(3,10))	0.6638	0.7247	0.7308	0.6280	0.6135	0.5429	0.6735	0.4931	0.6384	0.4961
	DTLZ5(5,10)	0.7186	**0.6846**	**0.6368**	**0.5908**	**0.5584**	**0.5230**	**0.5250**	**0.5409**	**0.6246**	0.5814
	600 (DTLZ5(3,10))	0.6863	0.7164	0.7285	0.6008	0.6147	0.5226	0.6510	0.5037	0.6105	0.5010
	DTLZ5(5,10)	0.6930	**0.6201**	**0.6365**	0.7071	**0.5527**	**0.5251**	**0.5307**	0.5915	**0.6025**	0.5793
	800 (DTLZ5(3,10))	**0.6681**	**0.6840**	0.6810	0.5904	0.6003	**0.5136**	**0.5509**	**0.5025**	0.7205	0.4947
	DTLZ5(5,10)	**0.6885**	0.6380	**0.6380**	0.6912	**0.5175**	**0.5248**	**0.5288**	0.5841	0.5936	**0.5375**
	900 (DTLZ5(3,10))	0.6992	0.7003	0.6337	0.5604	0.5942	0.5287	0.5482	0.5698	**0.4428**	0.4719
	DTLZ5(5,10)	**0.6127**	0.6515	0.6447	0.6530	0.5114	0.5189	0.5995	0.5659	0.5730	0.5213
	1000 (DTLZ5(3,10))	0.6825	0.6990	0.6295	0.5561	0.5883	0.5162	0.5214	0.5378	0.4516	0.4436
	DTLZ5(5,10)	0.6295	0.6521	0.6417	0.6174	0.5119	0.5173	0.5583	0.5530	0.5682	0.4632

the adaptability of E-dyNSGA-III to constant changes in the DMOP over 1,152, 576, 384, and 192 different time slots, respectively.

In this study, we analyze the performance of E-dyNSGA-III using the hypervolume Sharpe ratio (HSR) indicator [26]. The HSR indicator is an instance of the Sharpe ratio indicator in which the expected return and return covariance matrix are expressed with respect to the hypervolume (HV) indicator. The Sharpe ratio balances risk by ensuring that a given EA selects an optimal PF based on an appropriate reward-to-volatility ratio. Like all quality indicators, used in the selection or performance assessment of EAs, the HSR indicator is weakly monotonic. For a non-empty set of assets $A = \{a^{(1)}, \ldots.., a^{(n)}\}$, the global solution $x \subset \mathbf{X}$, which satisfies the reward-to-volatility ratio, is obtained according to

$$\max_{x \in [0,1]^n} g(x) = \frac{\Delta^T x - \Delta_b}{\sqrt{\left(x^T Q_x\right)}}, \tag{9}$$

where $\Delta \epsilon \mathbb{R}^n$ is a vector representing expected returns of A, Q is the covariance matrix of asset returns, $\mathbf{X}$ is the investment vector such that $X \epsilon [0,1]^n$, and r_b is the return of baseline riskless asset.

Desirable properties of the HSR indicator compared with the conventional HV indicator include monotonicity, non-degeneracy, and optimal investment and placement of

Table 6: HSR indicator values for the power generation model considering 4 different time windows (standard deviation in parentheses).

Time window (T_w) (mins)	Feature evaluation (FE)	dyNSGA-III	E-dyNSGA-III
5	500	1.135E-02(1.121E-01)	**1.478E-03(4.217E-02)**
	1000	2.459E-02(1.882E-02)	**3.387E-03(2.217E-02)**
	5000	2.617E-01(2.239E-01)	**3.214E-02(3.215E-01)**
	10000	3.698E-02(3.294E-01)	**2.483E-03(2.783E-02)**
10	500	2.350E-02(3.583E-02)	**3.618E-03(3.297E-02)**
	1000	1.884E-01(1.487E-02)	**3.506E-02(3.218E-02)**
	5000	4.205E-01(3.502E-01)	**2.515E-03(2.474E-02)**
	10000	**3.294E-03(4.215E-02)**	2.612E-02(3.217E-02)
15	500	**3.195E-02(2.386E-02)**	3.598E-02(3.218E-01)
	1000	2.504E-01(3.508E00)	**2.579E-02(5.215E-01)**
	5000	3.582E-01(2.712E-01)	**2.191E-02(2.575E-02)**
	10000	2.698E-01(3.583E-02)	**1.578E-03(3.215E-02)**
30	500	3.195E-01(2.386E-01)	**2.185E-03(2.356E-01)**
	1000	4.217E-01(3.206E00)	**3.219E-02(3.570E-01)**
	5000	**3.905E-02(2.496E-01)**	2.123E-01(4.129E-02)
	10000	2.217E-01(2.486E-01)	**4.213E-03(3.298E-02)**

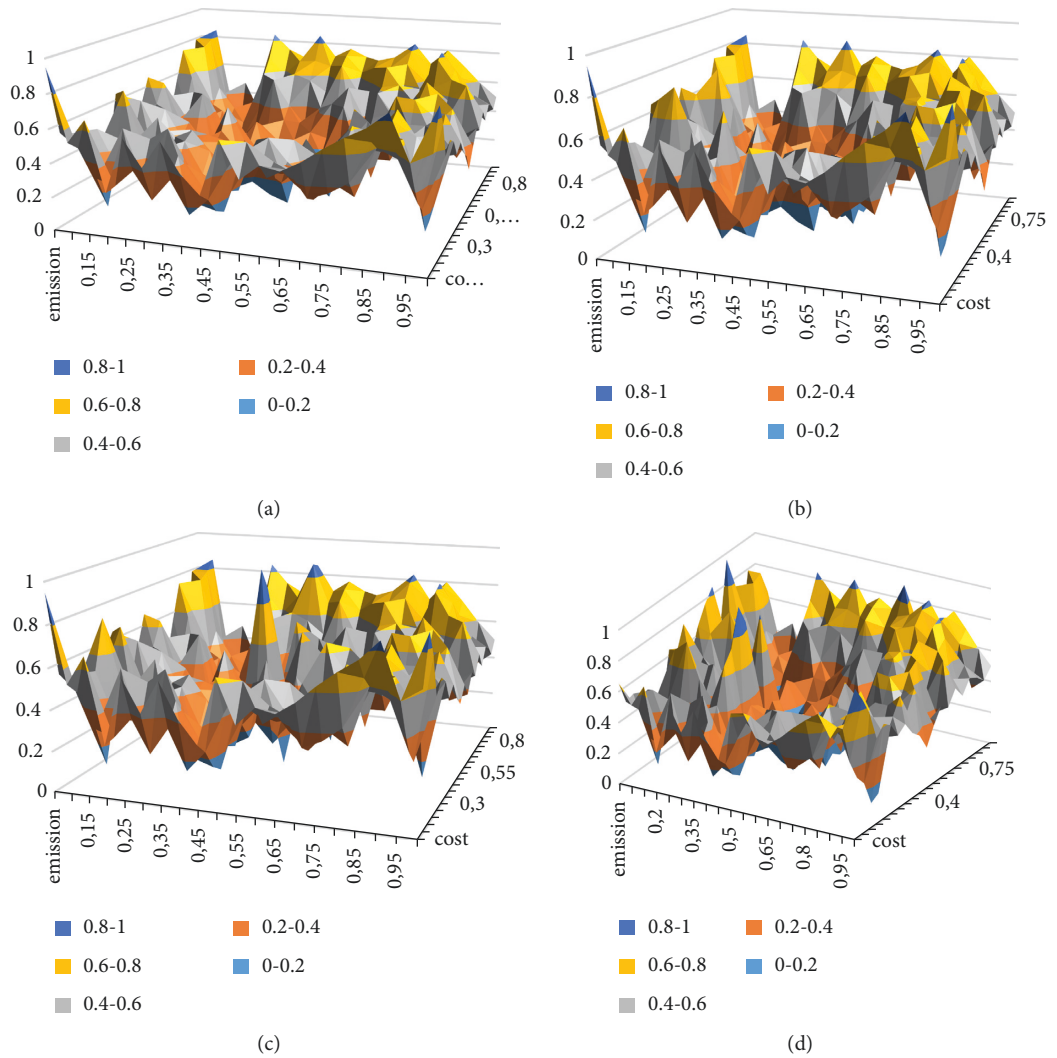

Figure 2: Surface plots for cost and emission objectives for E-dyNSGA-III for (a) 500 feature evaluations, (b) 1,000 feature evaluations, (c) 5,000 feature evaluations, and (d) 10,000 feature evaluations.

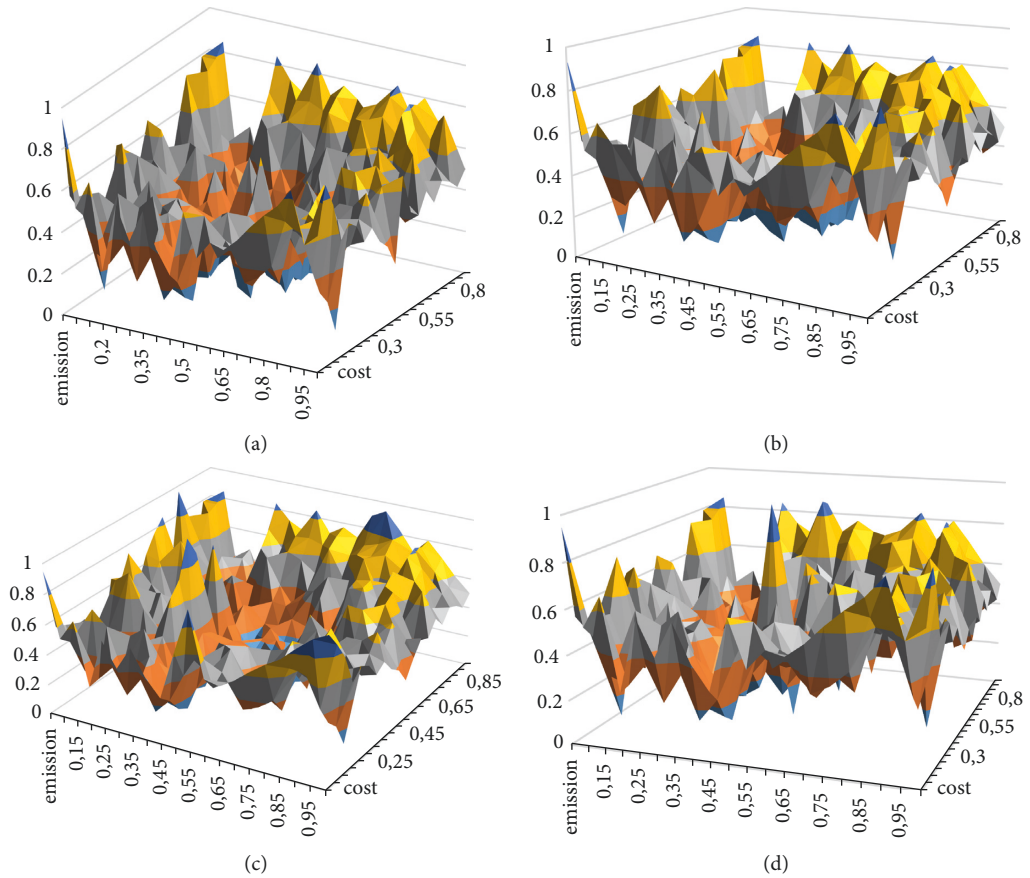

Figure 3: Surface plots for cost and emission objectives for dyNSGA-III for (a) 500 feature evaluations, (b) 1,000 feature evaluations, (c) 5,000 feature evaluations, and (d) 10,000 feature evaluations.

reference points [26]. Consequently, the HSR indicator requires less parameter settings than the HV indicator. Also, since it assigns zero investment to dominated solutions and strictly positive investment to non-dominated solutions, the possibility of a strictly non-dominated front is more likely. Further details on the formulation and performance of the HSR indicator can be found in [26].

3.5. Results on Performance of E-dyNSGA-III on Multi-Objective Hybrid Power Generation Scheduling Model. In this section, we will analyze the performance of the proposed algorithm on the optimization of the dynamic, hybrid power generation scheduling model introduced in Section 3.4. The purpose of this analysis is twofold. First, we want to observe how E-dyNSGA-III selects non-dominated solutions using the reference point-based HSR indicator. The dynamic nature of the DMOP will enable us to examine how the PF changes with corresponding changes in the time window of the DMOP. Second, we want to observe the capability of the proposed DMOEA to be used in real-time decision-making based on how quickly it responds to changes in the problem objectives and constraints. This is important because EAs generally perform better on static problems compared with time-varying problems. However, many real-world problems are dynamic, and the robustness of DMOEAs is greatly dependent on their capability to track time-varying PFs.

Figures 2 and 3 show surface plots for normalized values representing the cost and emission objectives of the DMOP. We compare the performance of E-dyNSGA-III with dyNSGA-III for 4 instances of feature evaluations (FEs): 500, 1,000, 5,000, and 10,000. The aim is to observe the capability of the DMOEAs to settle on the least expensive compromise between the cost and emission objectives for the generation model. From the figures, normalized values between 0 and 0.2 represent the best compromise between the two objectives. From the surface plots, we observe that dyNSGA-III exhibits higher peaks in the OF space compared with E-dyNSGA, particularly as the number of feature evaluations increases. This means that dyNSGA-III is likely to find it difficult to settle on the least expensive compromise between the two objectives. We also observe that E-dyNSGA-III concentrates the least expensive solutions in the center of the OF space, which is not the case with dyNSGA-III. The E-dyNSGA-III algorithm has a relaxed landscape at the center of the OF space compared with dyNSGA-III. The latter is characterized by peaks, which shows that dyNSGA-III finds it

challenging to settle on the least expensive set of solutions particularly when the number of feature evaluations is high. For 500 feature evaluations, dyNSGA-III is able to find a set of suitable solutions near the center of the OF space. However, as the number of feature evaluations increases, it becomes difficult for the algorithm to converge on a suitable

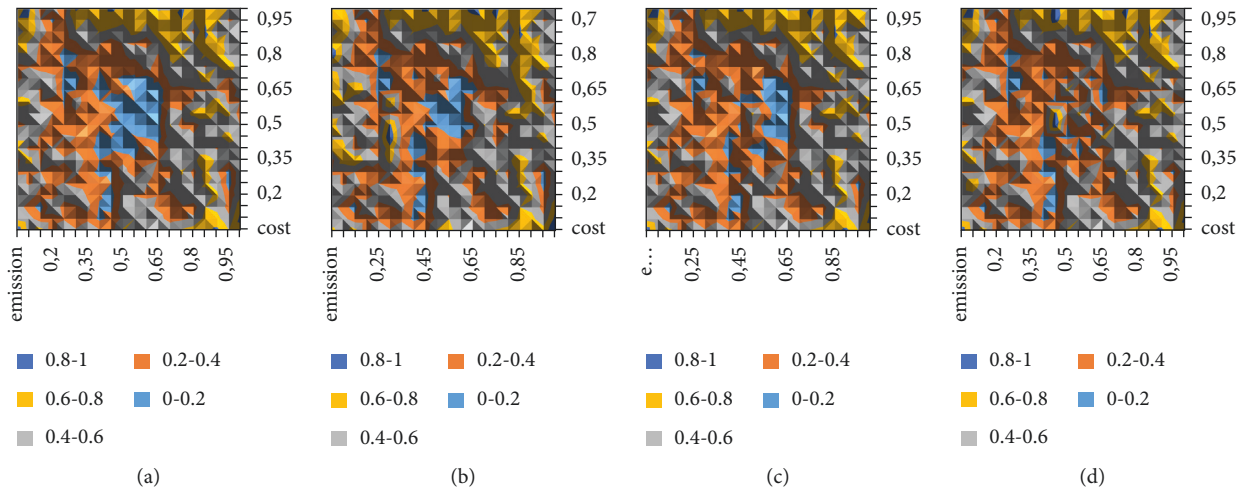

Figure 4: Contour plots for cost and emission objectives for (a) E-dyNSGA-III for 500 feature evaluations, (b) 10,000 feature evaluations, (c) dyNSGA-III for 500 feature evaluations, and (d) 10,000 feature evaluations.

set of reference points. It is important for DMOEAs to have the capability to track changes in the dynamic OF space since this is the basis for the real-world application of these algorithms. In this study, we consider two objectives with time-varying parameters and constraints. However, many real-world problems have more than two objectives. Therefore, satisfying the first aim of this analysis as detailed at the beginning of this section is vital.

In Figure 4, we analyze the ability of E-dyNSGA-III to be used in real-time decision-making by finding a feasible compromise between the cost and emission objectives. In Figures 4(a) and 4(b), we see the contour plots of E-dyNSGA-III for 500 and 10,000 feature evaluations, respectively. For both FE settings, we see that E-dyNSGA-III is able to settle on cheap solutions as seen by the concentration in the center of the plot. It can be seen that

more expensive solutions are concentrated at the edges of the plot. This is seen less in the plots of dyNSGA-III, particularly in the case of 10,000 FEs (Figure 4(d)). In this plot, there are almost no cheap solutions, which effectively balance cost and emission objectives of the DMOP. This difficulty to arrive at suitable solutions in the face of rapidly changing objectives, parameters, and constraints is one key reason why DMOEAs are limited in their application to optimization of real-world problems.

E-dyNSGA-III attempts to remedy this problem by the use of a niche of mutated solutions introduced into the candidate space. The effect of this approach is further investigated by comparing the performance of E-dyNSGA-III with dyNSGA-III using the HSR performance indicator. From Table 5, we see that E-dyNSGA-III is the best performer for 4 settings of the feature evaluations. We observe that the inclusion of mutated solutions causes more efficient placement of reference points, and consequently, a non-dominated PF is selected based on an appropriate reward-to-volatility ratio.

4. Conclusions

This study has proposed an archive approach using mutated solutions for assigning reference points based on an earlier proposed method for improving the capability of NSGA-II and NSGA-III to handle MOPs. We extend this approach to dynamic multi-objective optimization problems by improving the capability of earlier proposed dyNSGA-III to keep track of fit solutions in changing space and time.

When the number of objectives describing a DMOP is 3 or more, the dimensionality of the objective function space becomes complicated. This poses a challenge to the DMOEA as it struggles to maintain suitable candidate solutions throughout the search period. In particular, NSGA-III experiences a loss of selection pressure when the number of objectives and consequently the number of dimensions increase. We also observed this behavior with dyNSGA-III.

Therefore, in this study, we use an archive to preserve fit solutions when the number of objectives is 3 or more. This approach of using an archive of elite solutions in cases where the number of objectives is 3 or more is the attribute that distinguishes E-dyNSGA-III from the earlier proposed dyNSGA-III. To determine the rate of change in the given problem solution space, we consider the Minkowski distance $D_M(x, y)$ of solution a from its associated reference point at time t_n and t_{n+1}, respectively. If the change in $D_M(x, y)$ is large, then rate of change is large for solution a. Otherwise, the rate of change is considered to be small. For a small rate of change in the presence of 3 or more objectives, we infer that more competition is required to obtain the fittest candidates. Therefore, we introduce a larger proportion of mutated solutions according to the number of reference points. For instance, if a small change is detected, we introduce 2^M mutated solutions for every reference point. Otherwise, if the change is large, we increase the number of

reference points by $2^M - 1$ to guide the population to Pareto optimality. This strategy is what differentiates E-dyNSGA-III from dyNSGA-III. We tested the performance of the improved E-dyNSGA-III on four DMOPs with a complicated Pareto front. Preliminary results show that the proposed approach outperforms the original dyNSGA-III. Also, E-dyNSGA-III was able to associate a larger percentage of final candidate solutions with at least one reference point compared with dyNSGA-III, which indicates that the search strategy uses reference points to guide the solution space towards Pareto optimality. We also compared the performance of dyNSGA-III and E-dyNSGA-III on a real-world power generation scheduling model. We recognize the need to apply our DMOEA to optimize real-world problems. These algorithms are limited in practical applicability due to their inability to adapt to real-time changes in problem objectives, parameters, and constraints. Consequently, these algorithms get trapped in dynamic environments, which makes their performance unreliable. From the results obtained, the performance of E-dyNSGA-III is promising. However, we observe that for a large number of feature evaluations (5,000–10,000), there is a tendency for our proposed algorithm to get trapped in local optima. The real-world problem considered here has two objectives. Therefore, we ask ourselves the question: what happens when the number of objectives is more than two in the presence of many FEs?

Future work would focus on testing the performance of E-dyNSGA-III on DMOPs with more than 3 objectives with many dynamic feature evaluations. We observe that the proposed DMOEA optimizes multimodal, many-objective RPOOT problems satisfactorily. However, adapting it to perform satisfactorily on dynamic, real-world problems is still a work in progress. Particularly, when the number of objectives is 10 or greater, the number of reference points increases significantly, which can result in an increase in the processing time of the proposed algorithm. We are currently working to find a trade-off between accuracy and speed of the algorithm. Section 3.3 discusses the performance of E-dyNSGA-III on dimensionality reduction DMOPs, which is a test of its ability to reduce the number of redundant objectives in many-objective scenarios. However, more research is required to be able to train the algorithm to effectively handle such complex search environments. Satisfactory performance would demonstrate that E-dyNSGA-III can be used to effectively optimize a variety of real-world problems.

Data Availability

No data were used to support this study.

Conflicts of Interest

The authors declare that they have no conflicts of interest.

Acknowledgments

This research was supported partially by South African National Research Foundation Grants (Nos. 141951, 132159, 137951, and 132797).

References

[1] K. Deb, A. Pratap, S. Agarwal, and T. Meyarivan, "A fast and elitist multiobjective genetic algorithm: nsga-II," *IEEE Transactions on Evolutionary Computation*, vol. 6, no. 2, pp. 182–197, 2002.

[2] K. Deb and H. Jain, "An evolutionary many-objective optimization algorithm using reference-point-based nondominated sorting approach, part i: solving problems with box constraints," *IEEE Transactions on Evolutionary Computation*, vol. 18, no. 4, pp. 577–601, 2014.

[3] I. O. Essiet and Y. Sun, "Tracking variable fitness landscape in dynamic multi-objective optimization using adaptive mutation and crossover operators," *IEEE Access*, vol. 8, pp. 188927–188937, 2020.

[4] Y. Guo, H. Yang, M. Chen, J. Cheng, and D. Gong, "Ensemble prediction-based dynamic robust multi-objective optimization methods," *Swarm and Evolutionary Computation*, vol. 48, pp. 156–171, 2019.

[5] Y. Chi, Y. Xu, and R. Zhang, "Many-objective robust optimization for dynamic VAR planning to enhance voltage stability of a wind-energy power system," *IEEE Transactions on Power Delivery*, vol. 36, no. 1, pp. 30–42, 2021.

[6] A. Salimi and D. A. Lowther, "Projection-based objective space reduction for many-objective optimization problems: application to an induction motor design," in *Proceedings of the 2016 IEEE Conference on Electromagnetic Field Computation (CEFC)*, p. 1, Miami, FL, USA, November. 2016.

[7] A. Toktas and D. Ustun, "A triple-objective optimization scheme using butterfly-integrated ABC algorithm for design of multilayer RAM," *IEEE Transactions on Antennas and Propagation*, vol. 68, no. 7, pp. 5602–5612, 2020.

[8] B. Wang, H. Xie, X. Xia, and X. Zhang, "A NSGA-II algorithm hybridizing local simulated-annealing operators for a Bicriteria robust job-shop scheduling problem under scenarios," *IEEE Transactions on Fuzzy Systems*, vol. 27, no. 5, pp. 1075–1084, 2019.

[9] W. Liu, S. Gao, and L. H. Lee, "A multi-objective perspective on robust ranking and selection," in *Proceedings of the 2017 Winter Simulation Conference (WSC)*, pp. 2116–2127, Las Vegas, NV, USA, December. 2017.

[10] G. Sun, G. Li, S. Xia, M. Shahidehpour, X. Lu, and K. W. Chan, "ALADIN-based coordinated operation of power distribution and traffic networks with electric vehicles," *IEEE Transactions on Industry Applications*, no. 5, pp. 5944–5954, 2020.

[11] W. Hu, G. G. Yen, and G. Luo, "Many-objective particle swarm optimization using two-stage strategy and parallel cell coordinate system," *IEEE Transactions on Cybernetics*, vol. 47, no. 6, pp. 1446–1459, 2017.

[12] A. Panichella, F. M. Kifetew, and P. Tonella, "Automated test case generation as a many-objective optimisation problem with dynamic selection of the targets," *IEEE Transactions on Software Engineering*, vol. 44, no. 2, pp. 122–158, 2018.

[13] B. Cao, J. Zhao, Z. Lv et al., "Distributed parallel particle swarm optimization for multi-objective and many-objective large-scale optimization," *IEEE Access*, vol. 5, pp. 8214–8221, 2017.

[14] Z. Han, F. Liu, C. Xu, K. Zhang, and Q. Zhang, "Efficient multi-objective evolutionary algorithm for constrained global optimization of expensive functions," in *Proceedings of the 2019 IEEE Congress on Evolutionary Computation (CEC)*, pp. 2026–2033, Wellington, New Zealand, June 2019.

[15] A. Ibrahim, S. Rahnamayan, M. V. Martin, and K. Deb, "EliteNSGA-III: an improved evolutionary many-objective

optimization algorithm," in *Proceedings of the 2016 IEEE Congress on Evolutionary Computation (CEC)*, pp. 973–982, Vancouver, BC, Canada, July 2016.

[16] M. Farina, K. Deb, and P. Amato, "Dynamic multiobjective optimization problems: test cases, approximations, and applications," *IEEE Transactions on Evolutionary Computation*, vol. 8, no. 5, pp. 425–442, 2004.

[17] A. D. Manriquez, G. T. Pulido, and J. G. R. Torres, "Handling dynamic multiobjective problems with particle swarm optimization," in *Proceedings of the 2nd International Conference on Agents and Artificial Intelligence (ICAART 2010)*, pp. 337–342, Valencia, Spain, January 2010.

[18] Z. Zhang and S. Qian, "Artificial immune system in dynamic environments solving time-varying non-linear constrained multi-objective problems," *Soft Computing*, vol. 15, no. 7, pp. 1333–1349, 2011.

[19] Z. Zhang, M. Liao, and L. Wang, "Immune optimization approach for dynamic constrained multi-objective multimodal optimization problems," *American Journal of Operations Research*, vol. 02, no. 02, pp. 193–202, 2012.

[20] Y.-X. Li, Z.-H. Zhan, H. Jin, and J. Zhang, "Cloudde-based distributed differential evolution for solving dynamic optimization problems," in *Proceedings of the 10th International Conference on Intelligent Control and Information Processing*, pp. 94–99, Marrakesh, Morocco, December2019.

[21] J. D. Knowles and D. W. Corne, "Approximating the nondominated front using the Pareto archived evolution strategy," *Evolutionary Computation*, vol. 8, no. 2, pp. 149–172, 2000.

[22] M. López-Ibáñez, J. Knowles, and M. Laumanns, "On sequential online archiving of objective vectors," , Springer, Berlin, Heidelberg, 2011pp. 46–60, Lecture Notes in Computer Science.

[23] S. Biswas, S. Das, P. N. Suganthan, and C. A. C. Coello, "Evolutionary multiobjective optimization in dynamic environments: a set of novel benchmark functions," in *Proceedings of the 2014 IEEE Congress on Evolutionary Computation (CEC)*, pp. 3192–3199, Beijing, China, July 2014.

[24] R. Shang, K. Zhang, L. Jiao, W. Fang, X. Zhang, and X. Tian, "A novel algorithm for many-objective dimension reductions: Pareto-PCA-NSGA-II," in *Proceedings of the 2014 IEEE Congress on Evolutionary Computation (CEC)*, pp. 1974–1981, Beijing, China, July. 2014.

[25] M. Basu, "A simulated annealing-based goal-attainment method for economic emission load dispatch of fixed head hydrothermal power systems," *International Journal of Electrical Power & Energy Systems*, vol. 27, no. 2, pp. 147–153, 2005.

[26] A. P. Guerreiro and C. M. Fonseca, "An analysis of the Hypervolume sharpe-ratio indicator," *European Journal of Operational Research*, vol. 283, no. 2, pp. 614–629, 2020.